MATHEMATICA MONTISNIGRI
Vol LIII (2022)

MULTIGRID METHOD FOR NUMERICAL MODELLING OF HIGH TEMPERATURE SUPERCONDUCTORS

O.B. FEODORITOVA, M.M. KRASNOV, N.D. NOVIKOVA, V.T. ZHUKOV*

Keldysh Institute of Applied Mathematics, RAS. Moscow, Russia

*Corresponding author. E-mail: vic.zhukov@gmail.com

DOI: 10.20948/mathmontis-2022-53-7

Summary. An approach to numerical simulation of three-dimensional electrical and thermal fields in high-temperature superconductors is described. In such a semiconductor, the phenomena of superconductivity are observed at high temperatures above the temperature of liquid nitrogen. The absence of a generally accepted theory of superconductivity leads to the need to study physical processes in semiconductor structures using mathematical simulations. The main attention is paid to the calculation of temperature and electric current distributions in large-size mesas with a self-heating effect. An efficient algorithm for solving the equations describing these distributions is constructed. The basis of the algorithm is an adaptive multigrid method on structured Cartesian grids. The adaptability is based on the Chebyshev iterative method for constructing the smoothing procedures at each grid level and for solving the coarsest grid equations. The adaptive technique allows us to realistically simulate the anisotropic phenomena. The functionality of the algorithm is demonstrated along with an example of solving an anisotropic model problem with discontinuous coefficients.

1 INTRODUCTION

This paper is devoted to a problem of numerical simulation of three-dimensional electro-thermophysical processes in Bi-2212 semiconductors. In such a high-temperature semiconductor (HTS), the phenomena of superconductivity are observed at high temperatures above the temperature of liquid nitrogen, 77 K.

The absence of a generally accepted theory of superconductivity leads to the need to study physical processes in semiconductor structures using three-dimensional numerical simulations. In the Bi-2212 the superconducting and dielectric layers form anisotropic structure with Josephson mechanism of the electric current through non-conducting zones. The self-heating effect of the Bi-2212 is intensively studied; see for instance [1–5]. In the past decade, significant progress has been achieved by the high-temperature superconducting modelling community [6] to develop computational models for scientific investigations and for constructing of practical engineering devices [7–14].

As a result, numerical simulation has been recognized as a powerful instrument for investigating the electrical and thermal behavior of superconductors, and of HTS in particular.

For development of robust computational technique, we consider a mathematical model that takes into account the nonlinear electrical and thermal interactions. The electrical and thermal processes are modeled by a system of two coupled nonlinear differential equations for the temperature and the electric field potential. Physical fields in superconductors are anisotropic and of different scale nature. This is because the coefficients of thermal

2010 Mathematics Subject Classification: 35K05, 65M55, 82D55.
Key words and Phrases: Numerical simulation, High-temperature superconductor, Self-heating effect.

conductivity and the electrical resistivity are highly anisotropic. These coefficients depend on the temperature and the spatial coordinates. We take into account some typical formulas for these coefficients and their temperature dependences.

Due to nonlinearities some local features can be created by current-conducting hot channels. It is evident that efficient numerical models are needed to simulate these complex anisotropic phenomena accurately, and a coupling of the temperature and electrical current is critical. Calculations of such phenomena require the use of detailed three-dimensional grids with the large number of nodes, up to $\sim 10^9$ for complicated HTS devices.

The computational model introduced here is enabling us to model anisotropic phenomena realistically. We numerically compute temperature and electrical current distributions in mesas by solving jointly the non-linear heat conduction and potential equations with the adaptive multigrid method.

For spatial discrete approximation we use a conventional seven-point discretization on non-uniform Cartesian grids. As a result of discretization and linearization, the initial boundary-value problem is reduced to a multiple calculations of the systems of the discrete elliptic equations.

For solving these discrete equations we propose to apply the adaptive multigrid method. A detailed presentation of this algorithm, which is a version of R.P. Fedorenko classical method [15– 17], can be found in [18–23]. The adaptive multigrid is based on the Chebyshev iterative method which is used for constructing smoothing procedures at each grid level and for solving the coarsest grid equations.

This adaptation procedure exploits the power method for an optimal Chebyshev polynomial. Convergence of such a power method is based on the property of Chebyshev polynomials to grow rapidly outside the segment of least deviation from zero. This approach provides an automatic adaptation during multigrid iterations.

Experimental and numerical researches of Josephson structures are carried out in Russian and foreign scientific centers. In the Keldysh Institute of Applied Mathematics such a study is being carried out on the initiative of Prof. V.M. Krasnov, an employee of the Laboratory of Experimental Physics of Condensed Matter, Stockholm University. He deeply involves in investigation of HTS structures, see [5, 9–13].

The paper is organized as follows. In Section 2 we introduce the mathematical model. In Section 3 the finite-volume discrete model is presented. In Section 4 we describe application of the adaptive multigrid method in relation to the considered problem. In Section 5 we demonstrate the efficiency of the adaptive multigrid method as standalone solver for the heat conduction equation with the constant highly anisotropic coefficients. The results of self-heating mesa computations are presented in Section 6. Some conclusions are given in the last section.

2 MATHEMATICAL MODEL

Inside a solid body, which is the parallelepiped $\Omega = \{(x^1, x^2, x^3) : l_\alpha^- \le x^\alpha \le l_\alpha^+,\ \alpha = 1,2,3\}$, for simplicity, consistent temperature and electric potential stationary distributions are searched. We denote a point (x^1, x^2, x^3) in three dimensional space $\mathbb{R}^3$ as x, and as well as (x, y, z).

We use non-stationary formulation of the problem: in the parabolic cylinder $r=(t,\ x)\in G=[t_0;\ t_f]\times\Omega$, $\Omega\subset\mathbb{R}^3$: the unsteady system of the coupled equations to find steady–state distributions T, φ is considered

$$\begin{aligned} c(T)\frac{\partial T}{\partial t} &= \nabla\cdot k(T)\ \nabla \mathrm{T} + \nabla\varphi\cdot\sigma(T)\ \nabla\varphi, \\ \frac{\partial\varphi}{\partial t} &= \nabla\cdot\sigma\nabla\varphi. \end{aligned} \tag{1}$$

Here $k(T)$ is the thermal conductivity tensor, $c(T)$ is the volumetric heat capacity and $\sigma(T)$ is the electrical conductivity tensor. Tensors $k(T)$ and $\sigma(T)$ are assumed to be diagonal with the elements κ_{xx}, κ_{yy}, κ_{zz} and σ_{xx}, σ_{yy}, σ_{zz} respectively. These elements are given functions of temperature and coordinates. We specify time interval as $[t_0;\ t_\infty]$, $t_0=0,\ t_\infty\to\infty$. In (1) the expression $\nabla\cdot\sigma\nabla\varphi$ reads as an inner product of vectors from $\mathbb{R}^3$. For an inner product in the space of grid functions we use a notation $(\cdot,\cdot)$.

At any time $t>t_0$, the functions $T(r)$ and $\varphi(r)$ satisfy to a boundary condition (BC) on the boundary Γ of the parallelepiped (on six faces $x_\alpha=l_\alpha^{\pm},\ \alpha=1,2,3$). A conventional combination of BC types is possible.

For the temperature, either the Neumann condition $\partial T/\partial n=0$ at all boundaries is set, or the Neumann condition is defined on the horizontal faces of the parallelepiped and the Dirichlet condition rest $T=T_B$ is set on the vertical faces. The Dirichlet condition simulates constant cooling at some given temperature T_B, for example, $T_B=10\ K$.

For the potential φ, the Neumann condition $\partial\varphi/\partial n=0$ at the vertical faces is set, and a constant potential is maintained at the horizontal faces, upper and lower ones, i.e., the Dirichlet conditions are specified.

$$\varphi(t,x^1,x^2,\ l_3^+)=+0.5U_0,\qquad \varphi(t,x^1,x^2,\ l_3^-)=-0.5U_0 \tag{2}$$

with a given value U_0. One can take $U_0=1$ V, for example.

At $t=t_0$, the initial conditions $\varphi(t_0,x^1,x^2,x^3)=\varphi_0,\ T=T_0$, where $\varphi_0,\ T_0$ are the given functions or given constants, for example, $T_0=T_B,\ \varphi_0=0$. One can take the linear distribution of the potential along the vertical coordinate z^3:

$$\varphi_0=\frac{U_0}{l_3^+-l_3^-}\left(z^3-l_3^+\right)+\frac{U_0}{2}$$

It is impossible to solve the equation for potential and for temperature independently, because the electrical conductivity $\sigma=\sigma(T)$ depends on the temperature significantly, and the intensity of heat release in a unit volume, i.e. the heat source $q=\nabla\varphi\cdot\sigma(T)\ \nabla\varphi$, is nonlinear function of T, φ. The function $q(T,\varphi)$ simulates the heating of a substance by an

electric current flowing in the sample. The presence of the time derivatives in the system (1) means that the stationary solution is computed by a time-stepping procedure.

For a model problem of HTS, the resistivity components ρ_{xx}, ρ_{yy}, ρ_{zz}, $Ohm \cdot m$, can be given in the form

$$\rho_{xx} = \rho_{yy} = \rho_0 \exp\left(\frac{300}{150+T}\right), \qquad \rho_{zz} = a_\rho \rho_{xx}. \tag{3}$$

The diagonal elements of the electrical conductivity tensor σ_{xx}, σ_{yy}, σ_{zz}, $Ohm^{-1} \cdot m^{-1}$, have the form $\sigma_{xx} = 1/\rho_{xx}$, $\sigma_{yy} = 1/\rho_{yy}$, $\sigma_{zz} = 1/\rho_{zz}$. The components of the thermal conductivity tensor κ_{xx}, κ_{yy}, κ_{zz}, $W m^{-1} K^{-1}$, are set for the model case in the form $\kappa_{xx} = \kappa_{yy} = k_0 T$, $\kappa_{zz} = \kappa_{xx}/k_1$ with some empirical parameters k_0, k_1. The empirical formulas for the electrical and thermal conductivities are presented in Section 6.

The volumetric heat capacity $c(T)$, $J/(m^3 K)$, of a superconductor is set as a function of temperature T and density ρ: $c(T) = c_0 \cdot T^2 \rho$, $c_0 = 10^{-3}$. This function is determined by the specific heat c_m, $J/(kg \cdot K)$, and density ρ: $c(T) = c_m(T) \cdot \rho$ for the superconductor Bi-2212, one can take the density $\rho = 6 \cdot 10^3 kg/m^3$.

The dependencies (3) are of a model nature. In the vicinity of the critical temperature $T_{crit} \approx 85\ K$ of the superconducting transition, the actual behavior of electrical conductivity, thermal conductivity and heat capacity is more complicated.

After finding the steady-state solutions T, φ we compute the electric field $E = -\nabla \varphi$ and the electrical current density vector

$$J = \sigma E = -\sigma \nabla \varphi. \tag{4}$$

There are semiconductor structures of different geometric complexity. A description of the realistic mesa-type Bi2212 can be found in [12].

In this paper, we focus on temperature and current distributions in mesas with a self-heating effect; see [1–7, 11]. It is difficult to experimentally obtain current and temperature distributions in mesas, therefore high performance computer simulation is required. For this purpose we develop an algorithm and computer code for numerical calculation of these distributions by solving the non-linear system (1).

In this paper we present the basic elements of our numerical model for the case of a rectangular parallelepiped. Below we briefly give a scheme of the adaptive multigrid algorithm on structured Cartesian grids, see [18–23].

3 DISCRETE MODEL

We consider a model mesa as a parallelepiped Ω of sizes $l_x \times l_y \times l_z$. Typical values are $l_x \approx 3$, $l_y \approx 1.5$, $l_z \approx 0.02$ and $l_x \approx 50$, $l_y \approx 50$, $l_z \approx 1$, μm, for small-size mesa and large-size mesa respectively. We map this parallelepiped into the unit cube $\Omega = [0;1]^3$ with corresponding scale of the coefficients of the governing system.

In Ω we introduce a Cartesian grid $\Omega_h = \{x_n \in \Omega,\ 0 \le n \le N\}$ with the grid boundary Γ_h. The grid Ω_h is non-uniform in each coordinate direction with the number of cells N_x, N_y, N_z respectively and depends on a parameter h which characterizes the average cell size. The grid nodes are denoted as (x_i, y_j, z_k), or (i, j, k), where $i = 0,..., N_x,\ \ j = 0,..., N_y,\ \ k = 0,..., N_z$.

The grid functions T, φ, the coefficients of equations, residuals of the equations and etc. are determined at the grid nodes of Ω_h. We construct a node-based discrete scheme with finite-volume method. For this purpose we integrate the original equations over each dual volume $[x_{i-1/2};\ x_{i+1/2}]\times[y_{j-1/2};\ y_{j+1/2}]\times[z_{k-1/2};\ z_{k+1/2}]$ associated with (i, j, k)–node excluding the Dirichlet type nodes. If a grid index goes beyond values $0,\ N_x,\ N_y,\ N_z$, then such an index takes the closest value from $i = 0,..., N_x,\ \ j = 0,..., N_y,\ \ k = 0,..., N_z$.

The areas of six faces of the dual cell (i, j, k) are denoted as $S_{i+1/2, j, k}$, $S_{i, j+1/2, k}$, $S_{i, j, k+1/2}$ and the cell volume is demoted as $V_{i, j, k}$. Evidently that $V_{i, j, k} = 0$ for the Dirichlet type nodes. The grid function space U_h is defined in the standard manner with the inner product

$$(u, w) = \sum_{i, j, k} u_{i, j, k} w_{i, j, k} V_{i, j, k},$$

and the corresponding grid L_2 – norm. Here, the sum is taken over all grid nodes.

On the space U_h we introduce the discrete operators L_h^T and L_h^φ which approximate the linear differential operators $L^T = -\nabla \cdot \kappa \nabla$ and $L^\varphi = -\nabla \cdot \sigma \nabla$ with the second order accuracy on smooth functions, taking into account the boundary conditions. Here, the coefficients κ, σ are known functions of the spatial coordinates and they are determined by the temperature from the lower time layer. In 3D space the operators L_h^T and L_h^φ are constructed using a finite-volume 7-point discretization. They are self-adjoint with non-negative eigenvalues. We suppose that some estimates for the bounds of the spectrum $\lambda_{min} \ge 0$ and λ_{max} of each operator are known; these estimates can be calculated in a few simple cases [24]. In general cases, an estimate for λ_{max} is obtained with Gershgorin's circle theorem for estimating the eigenvalues of a matrix [25].

We introduce the semi-discrete approximation of the initial-boundary value problem (1) in an operator form:

$$c \frac{\partial T}{\partial t} + L_h^T \cdot T = f, \tag{5}$$

$$\frac{\partial \varphi}{\partial t} + L_h^\varphi \cdot \varphi = g. \tag{6}$$

We assume that the boundary conditions are taken into account with the definition of the operators L_h^T, L_h^φ and the right-hand side functions f, g.

The values of a grid function u at the time layer t_m is denoted as u_m. The transition from the layer t_m to the layer $t_{m+1} = t_m + \tau$ can be implemented in different ways. We write the convenient first order implicit scheme for the system (5) –(6)

$$\frac{T_{m+1} - T_m}{\tau} + \frac{1}{c} L_h^T \cdot T_{m+1} = \frac{1}{c} f_m, \tag{7}$$

$$\frac{\varphi_{m+1} - \varphi_m}{\tau} + L_h^{\varphi} \cdot \varphi_{m+1} = g_m. \tag{8}$$

The right-hand sides in these equations are taking into account the Dirichlet boundary conditions in nodes adjacent to the Dirichlet type nodes. The grid function f_m includes the heat source

$$q_m = q(T_m, \varphi_m) = \nabla \varphi_m \cdot \sigma(T_m) \nabla \varphi_m, \tag{9}$$

which arises from Joule-heating effect.

This implicit linear scheme can be written as a system of two operator equations

$$\left(I + \tau \cdot C^{-1} L_h^T\right) T_{m+1} = T_m + \tau C^{-1} f_m,$$

$$\left(I + \tau \cdot L_h^{\varphi}\right) \varphi_{m+1} = \varphi_m + \tau g_m,$$

where I is the identity grid operator, $C = c(T_m) I$. We rewrite this system as two linear systems

$$A_h u_h = f_h, \tag{10}$$

$$B_h v_h = g_h. \tag{11}$$

The operators $A_h = \tau^{-1} I + C^{-1} L_h^T$ and $B_h = \tau^{-1} I + L_h^{\varphi}$ are $N \times N$ –matrices, u_h, v_h are the seeking functions, $f_h = \tau^{-1} T_m + C^{-1} f_m$, $g_h = \tau^{-1} \varphi_m + g_m$ are the given grid functions.

Each of the equations (10) and (11) can be solved separately at each time step. Recalculation of the source (9) at each time step, as well as the coefficients of thermal and electrical conductivities, couples these equations. For convenience of description, we rewrite each equation in a compact form

$$A u = f, \tag{12}$$

where A is a self-adjoint positive definite operator, corresponding to A_h or B_h.

We describe the spatial discretization of the governing equations using their representation in a more convenient form:

$$-\sum_{\alpha=1}^{3} \frac{\partial}{\partial x^{\alpha}} \left(A_{\alpha} \frac{\partial u}{\partial x^{\alpha}} \right) + A_0 u = f. \tag{13}$$

Here A_0, A_1, A_2, A_3, f are the given non-negative functions of coordinates $(x^1, x^2, x^3) \equiv (x, y, z)$. In a discrete model the coefficients A_0, A_1, A_2, A_3 are calculated at grid points. To calculate the fluxes, the coefficients A_1, A_2, A_3 are additionally calculated on the faces of the dual cells $\{i+\frac{1}{2}, j, k\}$, $\{i, j+\frac{1}{2}, k\}$, $\{i, j, k+\frac{1}{2}\}$, i.e. on the faces passing through the centers of the geometric mesh cells $[x_i; x_{i+1}]\times[y_j; y_{j+1}]\times[z_k; z_{k+1}]$ and the middle of the edges; denote these coefficients as $A_1^{i+1/2, j, k}$, $A_2^{i, j+1/2, k}$, $A_3^{i, j, k+1/2}$, respectively. Each of these coefficients is calculated as the harmonic mean of the corresponding nodal values.

One considers the discretization of the heat source (9)

$$q = \nabla\varphi \cdot \sigma(T)\, \nabla\varphi = \frac{\partial\varphi}{\partial x} \cdot \sigma_1 \frac{\partial\varphi}{\partial x} + \frac{\partial\varphi}{\partial y} \cdot \sigma_2 \frac{\partial\varphi}{\partial y} + \frac{\partial\varphi}{\partial z} \cdot \sigma_3 \frac{\partial\varphi}{\partial z} \equiv q_x + q_y + q_z . \qquad (14)$$

The grid approximation of the function q is calculated at all nodes, except the Dirichlet type node for the heat equation. In the considered case, the Dirichlet BC is given only at the faces $k = 0$ and $k = N_z$. For $\partial\varphi/\partial x$ in each grid node (i, j, k) with the index $0 < i < N_x$ we have

$$\frac{\partial\varphi}{\partial x} \simeq \frac{\varphi(x_{i+1}, y_j, z_k) - \varphi(x_{i-1}, y_j, z_k)}{x_{i+1} - x_{i-1}} .$$

Therefore for such a (i, j, k)–node

$$q_x \simeq \sigma_1\left(x_i, y_j, z_k\right) \cdot \left(\frac{\varphi(x_{i+1}, y_j, z_k) - \varphi(x_{i-1}, y_j, z_k)}{x_{i+1} - x_{i-1}} \right)^2 .$$

At the faces $i = 0$ and $i = N_x$ we have prescribed the BC $\partial\varphi/\partial x = 0$, therefore $q_x = 0$ at these faces. At the nodes $(0, j, k)$ and (N_x, j, k), the terms q_y and q_z are written in the same way. On the edges of the cube, which shares two faces with the Dirichlet and Neumann conditions, the Dirichlet condition has priority. The discretization of the terms q_y, q_z is the same in the interior nodes. At the faces $z = 0$ and $z = N_z$ we have prescribed the Dirichlet BC (2) for the potential and the Neumann BC for the temperature. Therefore the source function (14) must be computed at these faces. To provide such a procedure we discretize $\partial\varphi/\partial z$ by the convenient three-point difference derivatives with second order of accuracy.

For linear equations the implicit scheme does not require any restriction on time step size. But in our nonlinear case the choice of the time step size τ is limited by an empirical rule: the growth of the heat source $q = q(T, \varphi)$ must be restricted. We require $\|q_{m+1}\| < q_{tol}\, \|q_m\|$ for transition from the layer t_m to the layer $t_{m+1} = t_m + \tau$ with a given tolerance q_{tol}.

4 GENERAL SCHEME OF THE ADAPTIVE MULTIGRID METHOD

This section briefly presents the results of the development of the classical multigrid method [15-18, 21] in relation to the described problem. We assume that the system (12) is the result of the grid approximation of the boundary value problem for the equation (13). Various iterative methods are usually used to solve such a system. Size of these systems $N = N_x \times N_y \times N_z$ effects on the efficiency of the methods, and a value N can be very large. Additional difficulties arise from anisotropy, which is also characteristic of the problem under consideration (1).

For elliptic differential equations the multigrid method [15-17] is theoretically optimal: the computational complexity of the method grows linearly with an increase of unknowns. Its real efficiency depends on the implementation of the algorithmic elements. The main elements are intergrid transfer operators, smoothing operators and procedures for solving the coarsest grid equations. In this paper, we summarize the main elements of the multigrid method and the principle of automatic adaptation during multigrid iterations. Detailed information can be found in [18-23].

Every multigrid iteration step consists of the transition from a fine grid level to the next grid level up to the coarsest grid and back ($V-$cycle). It is convenient to represent the multigrid method in a two-grid representation, describing the transition from a fine h–grid to a coarse H – grid. We rewrite the initial system of discrete equations at a fine grid level as $A_h u_h = f_h$.

On the coarse grid level, a correction system in the form $A_H w_H = g_H$ is constructed. We construct the operator A_H with discretization on the H–grid. The right-hand side g_H is the constraint of the residual $g_h = f_h - A_h u_h$ on the coarse grid, i.e. $g_H = R g_h$. Here P and R are the interpolation and projection operators, they are conjugate, $R = P^*$. The operator P can be constructed with the trilinear interpolation. Along with a trilinear interpolation, we use an approximate solution of the local discrete boundary value problem. Such operators P and R provide a problem-dependent intergrid transfer and they provide robustness of the multigrid method for discontinuous coefficient equations, see [18].

In the two-grid representation the error propagation operator can be write as

$$Q = S_p (I - P A_H^{-1} R A_h) S_p , \tag{15}$$

where I is the identity operator, S_p is the smoothing operator. The given two-grid algorithm is recursively generalized to an arbitrary of grid levels.

Smoother procedure S_p plays a key role in the multigrid efficiency. We propose to construct an explicit iterative Chebyshev smoother providing the ability to adapt during the multigrid iterations, see [21, 22]. This adaptive smoother can be explained together with the coarsest grid solver for the linear system $A_H \cdot y = g_H$ with $g_H = R \cdot (g_h - A_h u_h)$.

For generality we consider a linear system (12) with self-adjoint and positive definite matrix A. To solve this system, one can apply the explicit Chebyshev iterative method [24]

$$u_j = u_{j-1} + \omega_j (f - A \cdot u_{j-1}) \tag{16}$$

with an optimal set of parameters $\{\omega_j\}$ and an initial guess u_0. Here $j=1,...,p$ is the iteration number, and p is a priori defined by the condition to reach a prescribed relative accuracy ε: $\|r_p\| < \varepsilon \|r_0\|$, where r_0 and $r_p = f - A\cdot u_p$ are the initial and final residuals. The number p depends on ε and the number $\eta = \lambda_{min}/\lambda_{max}$ according to the formula

$$p = p(\varepsilon,\eta) = \ln\left(\varepsilon^{-1} + \sqrt{\varepsilon^{-2}-1}\right) / \ln\left(\left(1+\sqrt{\eta}\right)/\left(1-\sqrt{\eta}\right)\right), \qquad (17)$$

where $0 < \lambda_{\min}$, $\lambda_{\max}$ are minimal and maximal eigenvalues of A. This well-known iteration procedure is defined by the Chebyshev polynomial F_p of degree p, that deviates least from zero on $[\lambda_{min};\lambda_{max}]$ and is normalized by the condition $F_p(0)=1$. The parameters ω_j, $j=1,...,p$ are reordered for computational stability [24].

We use notations λ_{min} and λ_{max} for the exact eigenvalues, λ^*_{min} and λ^*_{max} for their approximate estimates. The values λ_{min} and λ_{max} are usually unknown.

After running the algorithm (16), we obtain the relation $r_p = F_p(A)r_0$ for the initial and final residuals. To start the algorithm it is necessary to set the bounds λ^*_{min} and λ^*_{max} of the spectrum of operator A. The desired bound $\lambda^*_{max} \geq \lambda_{\max}$ is estimated with the Gershgorin theorem [25]. As an initial bound of eigenvalue λ^*_{min} the Rayleigh–Ritz ratio $\lambda^*_{min} = (Av,v)/(v,v)$ can be used, where v is the right-hand side of the linear system of equations. With adaptation any empirical upper estimate λ^*_{min} is appropriate.

The relations $0 < \lambda_{min} \leq \lambda^*_{min} \leq \lambda_{max} \leq \lambda^*_{max}$ are guaranteed the convergence of the method (16). The desired estimate is specified during the external iterative process (or adaptation cycle). Let λ^*_{min} be a current guess, and λ^*_{new} is its update. The adaptation algorithm has the following form. One needs to solve a linear system with a prescribed accuracy ε_{tot}, but firstly the lower accuracy value $\varepsilon_1 < \varepsilon_{tot}$ we set. For instance, $\varepsilon_{tot} = 10^{-10}$ and $\varepsilon_1 = 10^{-2}$. We implement one step of the Chebyshev algorithm with the given data λ^*_{min}, λ^*_{max}, ε_1 and obtain $\delta = \|r_p\| / \|r_0\|$ with $r_p = F_p(A)r_0$. Here $\delta \equiv \delta_k$ is an accuracy achieving in the current adaptation cycle with the number $k=1,....$, and r_0, r_p are the initial and final residuals. Assume that $\delta > \varepsilon_1$. Then the new update is found as the unique root of the algebraic equation $F_p(\lambda) = \delta$, therefore $\lambda^*_{min} = \arg(F_p(\lambda) - \delta = 0)$. If the accuracy ε_{tot} is not achieved, we pass to a new adaptation cycle with λ^*_{min}, λ^*_{max}, ε_1 and with the Chebyshev polynomial degree calculated by formula (17).

An accuracy $\delta = \delta_k \leq \varepsilon_1$ can be achieved at an adaptation step k. In general this means that the estimate λ^*_{min} is sufficiently accurate. Therefore we can perform the next step with

the previous data λ^*_{min}, λ^*_{max}, ε_1, or change the accuracy by setting $\varepsilon_1 = \varepsilon_{tot}/(\delta_1 \times .... \times \delta_k)$. With this choice, the desired accuracy ε_{tot} is achieved in one adaptation step.

This adaptation procedure exploits the power method for the polynomial $F_p(A)$ which is an eigenvalue algorithm: for $F_p(A)$ this algorithm produces a number λ, which is the greatest (in absolute value) eigenvalue: $\lambda = \lambda^F_{\max}$. Evidently that $\lambda^F_{\max} = F_p(\lambda_{\min})$. Convergence of such a power method is based on the property of Chebyshev polynomials to grow rapidly outside the segment of least deviation from zero.

This adaptation algorithm can be easily integrated into the multigrid method. It provides the efficiency of solving the coarsest grid system by refining the estimate λ^*_{min} and it is well suited for constructing an adaptive smoother at each grid level, see [21, 22]. The adaptive Chebyshev smoother serves to reduce the initial residual on the high-frequency part of the spectrum $[\lambda^c_{\min}; \lambda^*_{\max}]$. The high-frequency spectrum bound $\lambda^c_{\min}$ is unknown in advance and is found in adaptation process. Adaptation is turned on automatically if a relation $\delta = \| r_p \| / \| r_0 \| > \varepsilon_{smooth}$ is obtained on some grid level after the smoothing. This means that the given smoothing accuracy ε_{smooth} is not achieved. In this case, we refine the parameters of the smoothers using simple formulas, see [21, 22]. For example, for the Chebyshev smoother the parameters are updated according to the new boundary $\lambda^c_{\min}$ and the known upper boundary $\lambda^*_{\max}$.

After updating $\lambda^c_{\min}$ at all grid levels, multigrid iterations are continued with new values, repeating if necessary adaptation (while $\varepsilon_{smooth} < \delta < 1$). As a rule, in calculations after several (2–3) multigrid iterations the parameters of smoothing are stabilized, the specified accuracy of smoothing s_{smooth} is achieved, and the asymptotic convergence rate of the multigrid iterations becomes equal to the expected value ε^2_{smooth}.

The presented technique exploits the explicit iterations therefore this method is suitable for the efficient implementation on ultra-parallel computers with potential scalability on a large number of processors.

5 STANDALONE ADAPTIVE MULTIGRID SOLVER

The problem of calculating a HTS structure is characterized by a high difference in the geometric sizes of the domain, highly anisotropic parameters, and the grid anisotropy can deliver an additional difficulty.

Firstly we demonstrate the efficiency of the adaptive multigrid method as standalone solver for the equation (13) with constant highly anisotropic coefficients $A_1 = 10000,\ A_2 = 100,\ A_3 = 1,\ A_0 \equiv 0$ in the unit cube Ω with the Dirichlet boundary conditions and with uniform and non-uniform Cartesian grids. The convergence rates of the multigrid iterations are characterized by the relation $s = r_n / r_{n-1}$, where r_{n-1}, r_n are the grid norms of the residuals at two sequential multigrid iterations. The grid of cells $64 \times 64 \times 64$ is taken, the number of grid levels is 3, the grids of the next levels are $32 \times 32 \times 32$ and

$16\times16\times16$. In the experiments, grids are taken up to 2048^3 cells. We set the smoothing factor $\varepsilon_{smooth}=0.5$. So, we try to achieve the condition $d=r_{before}/r_{after}<\varepsilon_{smooth}$ for the ratio of residual norms before and after smoothing at any stage of smoothing. This goal is achieved with the adaptive refining of the spectrum bounds. The coarsest grid equations are solved with relative accuracy $ctol=10^{-3}$ using the Chebyshev adaptive method. Convergence of multigrid iterations is controlled by condition $r_m<\varepsilon_{tot}\cdot r_0$ with accuracy $\varepsilon_{tot}=10^{-14}$.

We compute this problem for two cases: using uniform and a non-uniform grids. Figure 1 demonstrates on a logarithmic scale the evolution of the residual norm and the convergence rate $s=r_n/r_{n-1}$, with respect to the number n of the multigrid iterations for a non-uniform grid. We use the geometric progression of mesh sizes in the vertical direction, so that the cell sizes in the vertical direction are equal to 0.1 for the lower and 10^{-4} for upper boundary of the unit cube respectively. For the both cases such graphics are practically similar. Adaptation works equally well. The computational costs are different: for the non-uniform grid CPU time increases by 25%. In terms of the number of smoothing iterations, the costs are 1100 and 1620 iterations totally. The residual norm during multigrid iterations decreases from the initial value 10^7 down to $\sim5\cdot10^{-8}$. Adaptation is turned on after the second multigrid iteration.

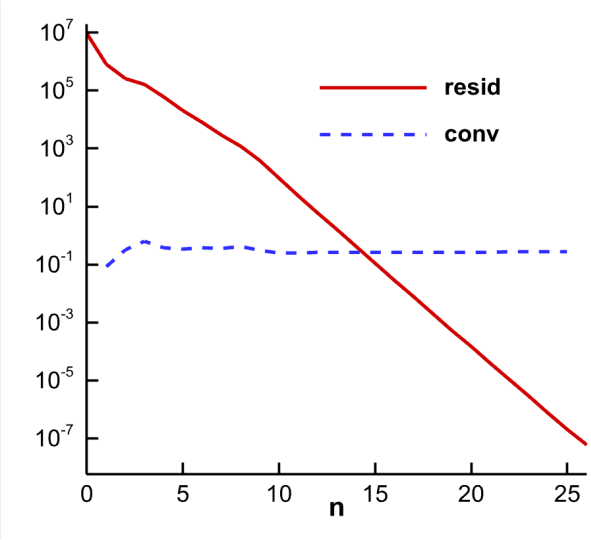

Fig. 1. Multigrid iterations: the residual norm (solid line) and the convergence rate (dashed line)

The convergence rate s (dashed lines in Figure 1) stabilizes during the first 5-7 iterations at $s=0.27$. It indicates that the multigrid asymptotic convergence rate is practically achieved. This value is close to the theoretical value $s=\varepsilon_{smooth}^2=0.25$. If we take the relative accuracy of coarsest grid solver as $ctol=10^{-9}$, the convergence rate s stabilizes at the theoretical value $s=\varepsilon_{smooth}^2=0.25$. The computational cost practically does not increase at the same time. For this case one can observe influence of adaptation: the computation time is reduced by 25%, and the total number of operations for calculating residuals also is reduced. For

parallel implementation, it is important to reduce the number of multigrid iterations, which leads to a reduction of global operations like calculating residual norms.

6 RESULTS OF SELF-HEATING MESA COMPUTATIONS

We are adjusting the statement of the considered initial boundary-value problem under the following assumptions. A computational domain is the unit cube. Since we are seeking for a steady-state distribution of electrical potential and temperature, we assume the volumetric heat capacity $c(T) \equiv 1$. All coefficients $\kappa(T)$, $\sigma(T)$ correspond to a conventional semiconductor microscale structure $l_x \times l_y \times l_z$. We map this parallelepiped into the unit cube and set the input data as

$$\begin{aligned} &T_0 = T_b = 10, \;\; U_0 = 1, \\ &\kappa_{xx} = \kappa_{yy} = 0.1 \cdot T, \;\; \kappa_{zz} = 50 \cdot \kappa_{xx}, \\ &\sigma_{xx} = \sigma_{yy} = \;\; 100 \cdot \exp\left(-300/\left(150 + T\right)\right), \end{aligned} \tag{18}$$

$$\sigma_{zz} = \begin{cases} 5 \cdot 10^{-1} \sigma_{xx}, & x \notin [0.375; \;\; 0.625], \\ 4 \cdot 10^{-3} \sigma_{xx}, & x \in [0.375; \;\; 0.625]. \end{cases} \tag{19}$$

We focus on discontinuity of the component σ_{zz}, see (19). This is an artificial introduction of a feature in order to demonstrate the capabilities of the method.

The boundary conditions (BCs) of the six faces of the cube can be written in the form:

$$\begin{aligned} &x = 0: \;\; \partial\varphi/\partial n = 0, \;\; T = T_b; \;\; x = 1: \;\; \partial\varphi/\partial n = 0, \;\; T = T_b, \\ &y = 0: \;\; \partial\varphi/\partial n = 0, \;\; \partial T/\partial n = 0; \;\; y = 1: \;\; \partial\varphi/\partial n = 0, \;\; \partial T/\partial n = 0, \\ &z = 0: \;\; \varphi = -0.5U_0, \;\; \partial T/\partial n = 0; \;\; z = 1: \;\; \varphi = +0.5U_0, \;\; \partial T/\partial n = 0. \end{aligned}$$

The initial data at $t = t_0$:

$$T = T_0(x, y, z) = T_B, \quad \varphi = \varphi_0(x, y, z) = U_0 \left(z - 1\right) + 0.5U_0.$$

We emphasize again this statement of the problem serves to demonstrate the methodological capabilities of our approach, and not to simulate a specific device. The 3D typical temperature distribution is shown on Figure 2.

If we take constant values for the heat and electrical conductivities, then a solution of the governing system has too simple an analytical representation: $T = 0.5\sigma_z \, x(1 - x), \quad \varphi = U_0 \left(z - 1\right) + 0.5U_0$. Using the resistivity components in the form (3) doesn't make the solutions complicated. To simulate a genuine non-trivial two-dimensional solution, we take the input data (18), (19) and in additional define the BC for the potential φ like a "hat" function on the down and upper faces $z = 0$ and $z = 1$. These conditions define as

$$\varphi(t, x, y, 0) = -0.5 \, U_0 \; - \; b \, f, \quad \varphi(t, x, y, 1) = +0.5 \, U_0 \; + \; b \, f,$$

at the faces $z = 0$ and $z = 1$ respectively. Here the function $f(x)$ is given by the formula

$$f = \begin{cases} 0.5(\tanh(a(x - 0.25)) + 1), & x < 0.5, \\ 1 - 0.5(\tanh(a(x - 0.75)) + 1), & x \geq 0.5. \end{cases}$$

Here a, b are free parameters, for instance $a = 40$, $b = 0.1$. We have $\varphi_x(t, x, y, 0) = b\, f_x = ab \cdot \mathrm{sech}^2(a\,(x - 0.25))$. Therefore $\max |\varphi_x(t, x, y, 1)| = ab$ and the solution becomes two-dimensional one. The plot of the function $\varphi(t, x, y, 1)$ with respect to x is shown on Figure 3. The function $\varphi(t, x, y, z)$ does not depend on y.

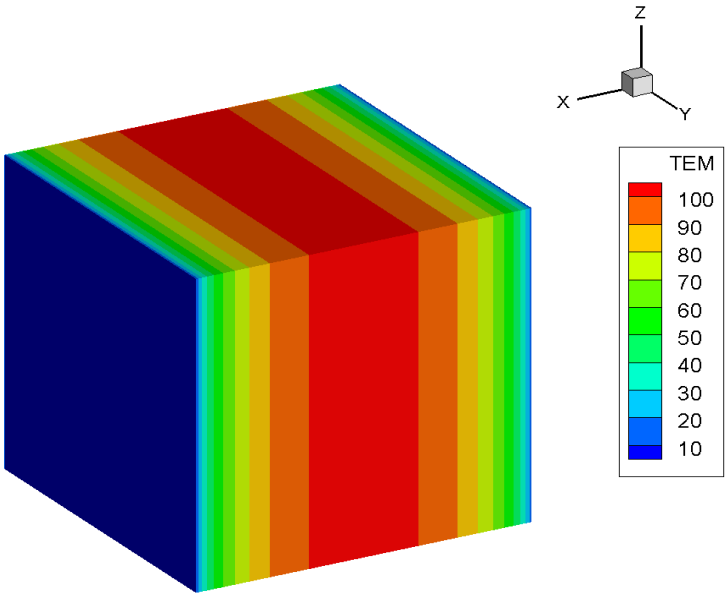

Fig. 2. A typical temperature distribution

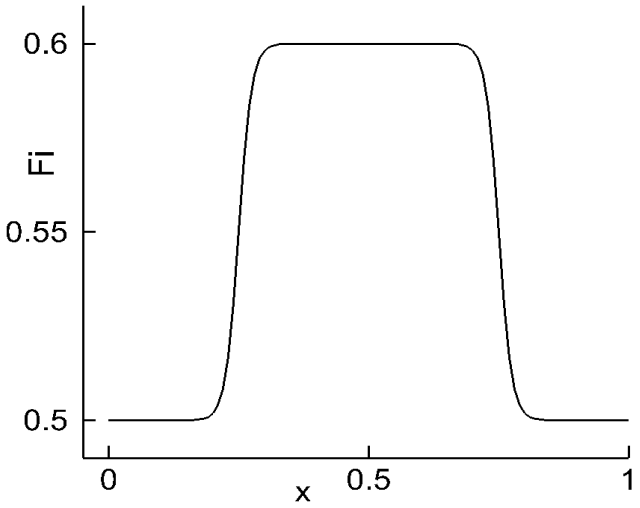

Fig. 3. The profile $\varphi(t, x, y, z)$ along Ox at the point $(z, y) = (1,\ 0.5)$

In computations we take a few grids with $N_x \times N_y \times N_z$ cells with $N_x = N_z = 128,\ 256,\ 512$. Since the sought solution does not depend on y we set $Ny = 3$.

A numerical solution which is obtained on the grid $512 \times 3 \times 512$ practically does not depend on the further grid refinement. Therefore we present the results on this most detailed grid. The parameters of the adaptive multigrid used to solve the implicit discrete system (7), (8) on each time level can be varied, but the results are given below for the following values: the four multigrid levels; the relative accuracy of the coarsest grid equations $ctol = 10^{-3}$; the smoothing factor $\varepsilon_{smooth} = 0.5$; the accuracy of the multigrid iterations $\varepsilon_{tot} = 10^{-6}$.

An initial time step size is $\tau_1 = 0.01$. In the time stepping we increase the time step size with $t_{m+1} = t_m + \tau_m$, $\tau_{m+1} = (m+1) \cdot \tau_m$, $m = 1, 2, \ldots$. As a result, a steady-state solution is achieved when $m > 10$. We control the solution stabilization in time with calculation of the norm of the grid functions $\Delta T_m = T_{m+1} - T_m$, $\Delta\varphi_m = \varphi_{m+1} - \varphi_m$. The evolution of the norm of ΔT_m, $\Delta\varphi_m$ is shown on Figure 4. At $m = 11$ the absolute values $\max|\Delta T_m| \approx 0.1$, $\max|\Delta\varphi_m| \approx 3 \cdot 10^{-7}$, i.e. the relative error of the time stepping process is less than 0.01 for temperature and less than 10^{-6} for potential. The difference in the errors has clear explanation: in the heat conduction equation, the source is discontinuous in correspondence with (19).

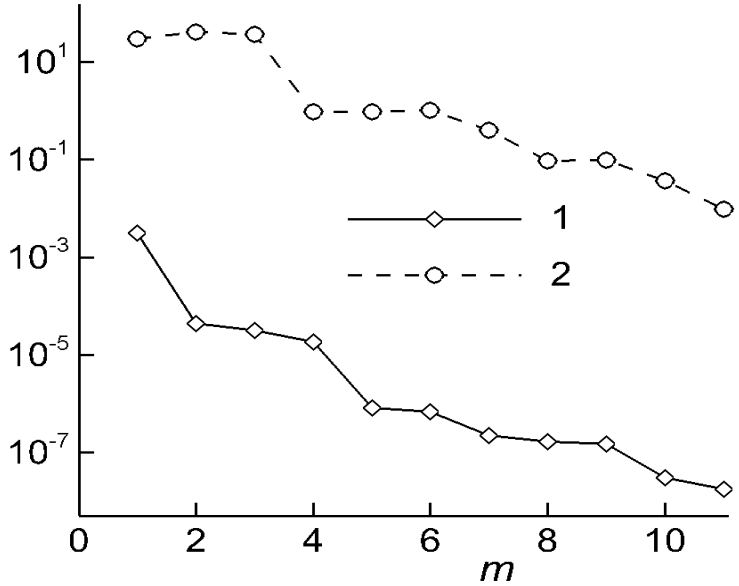

Fig. 4. The time evolution of the norm of $\Delta\varphi_m$ and ΔT_m: 1 and 2 respectively

The *Oxz* plane distribution of the potential is show on Figure 5. The profiles of the temperature and the vertical component *Jz* of the electrical current density vector (4) are given on Figure 6, 7 respectively. We show the profiles along *Ox* at the point $(z, y) = (0.5,\ 0.5)$. In the central part of the domain, in accordance with (19), there is no

Joule heating, the temperature of this zone achieves $T = 100\,K$ by the heating of this zone due to thermal conductivity.

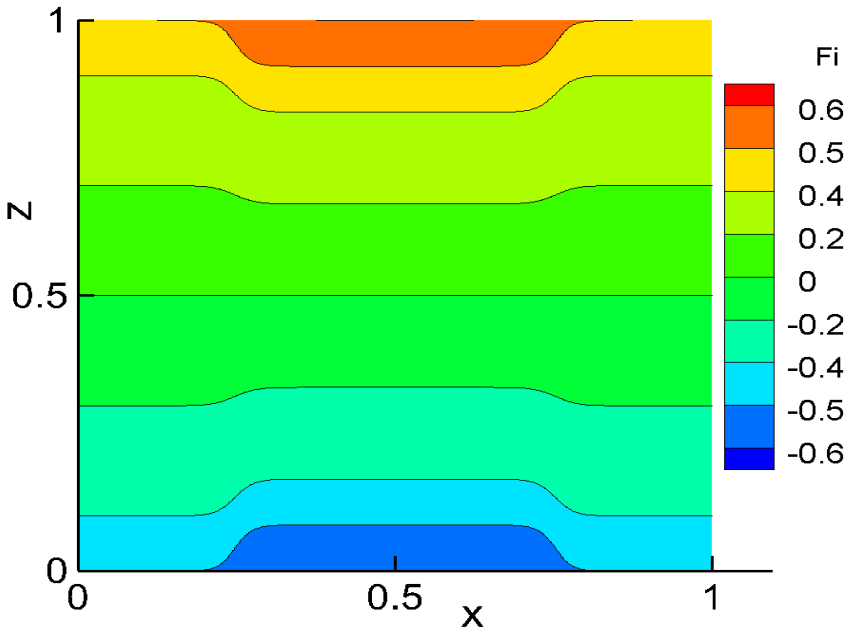

Fig. 5. Potential distribution in Oxz plane

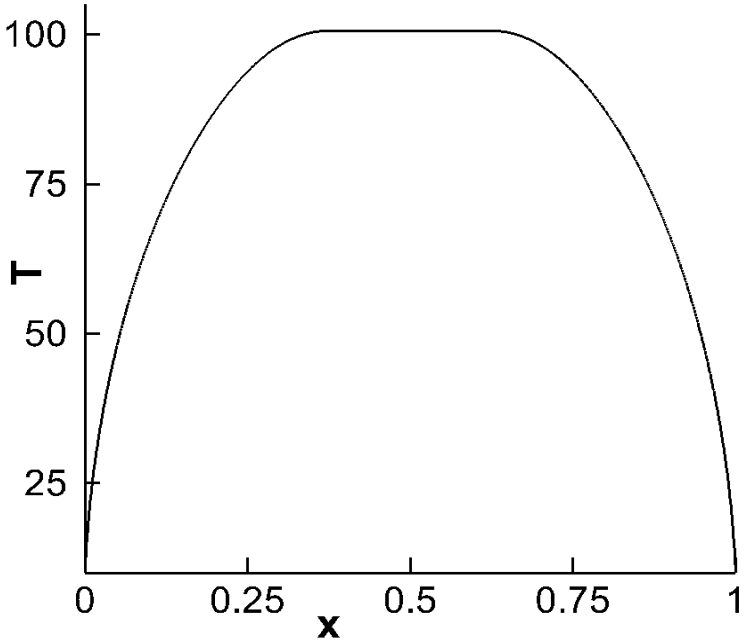

Fig. 6. Temperature: the profile along Ox at the point $(z, y) = (0.5,\ \ 0.5)$

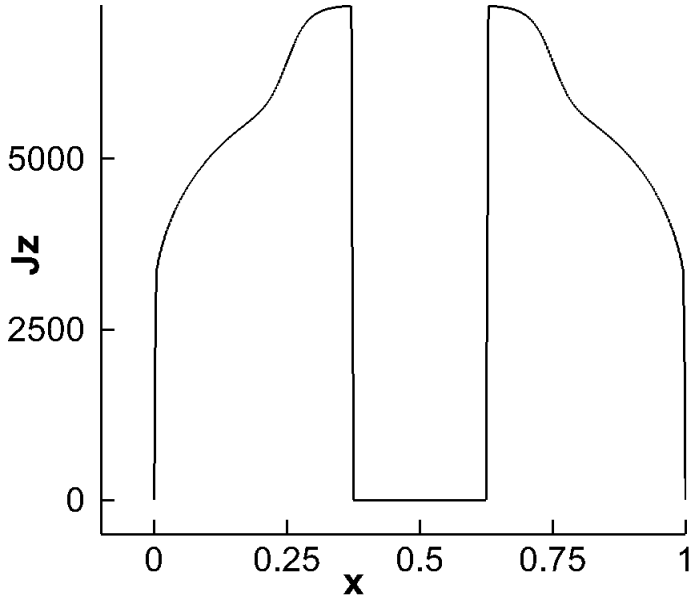

Fig. 7. The vertical component of the electrical current density vector: the profile along Ox at the point $(z, y) = (0.5,\ 0.5)$

The presented numerical results prove the efficiency of the proposed approach in solving problems with anisotropic discontinuous coefficients, which is typical for HTS problem.

7 CONCLUSION

In this work, an efficient approach to the numerical modelling of coupled electric and thermal fields in high-temperature superconductor (HTS) is developed. The absence of accurate knowledge of superconductivity leads to the need to study HTS structures using mathematical simulations. We have modeled heat transport and the resulting spatial temperature distribution in the presence of Joule self-heating due to electrical current in mesa material.

We have proposed a numerical technique to study temperature and current distributions in large-size mesas with a self-heating effect. The robust algorithm for solving the governing equations is constructed. The key element of the algorithm is an adaptive multigrid method on structured Cartesian grids. The adaptability allows us to realistically simulate the anisotropic phenomena that are typical for HTS problems. The numerical experiments show the robustness of the algorithm as standalone solver for highly anisotropic model problem as well as a solver for the system of two coupled nonlinear equations for the temperature and the electric field potential.

In the case of the usage of the multigrid algorithm as a standalone solver the adaptive approach allows us to achieve automatically the prescribed convergence rate. In the case of two coupled nonlinear equations the efficiency of the multigrid can be improved by analyzing and exploiting a convergence history in the solution process. For optimal incorporation of time-stepping information in the solution process further researches are needed.

The role of interconnections of thermal conductivity, electrical resistance and the device geometry are under investigations.

The adaptive method is suitable for the efficient implementation of the computer code on conformal block-structured grids with potential scalability on ultra-parallel computers with a large number of processors.

The proposed computational technique can be adopted for solving a similar problem, for instance a problem of thermal breakdown in solid dielectrics [26, 27].

Acknowledgements. The study was supported by Russian Foundation for Basic Research (project no. 19-01-00670 A).

REFERENCES

[1] D.Oikawa, H. Mitarai, H. Tanaka, K. Tsuzuki, Y. Kumagai, T. Sugiura, H. Andoh, and T.Tsukamoto, "Numerical analysis of temperature and current distributions in large-size intrinsic Josephson junctions with self-heating", *AIP Advances*, **10**, 085113 (2020). https:// doi.org/10.1063/5.0018989.

[2] A. Yurgens, "Temperature distribution in a large Bi2Sr2CaCu2O8+ δ mesa", *Phys.Rev. B*, **83**, 184501 (2011). https://doi.org/10.1103/PhysRevB.83.184501.

[3] Oliver M. G. Ward, Edward McCann, "The heat equation for nanoconstrictions in 2D materials with Joule self-heating", *J. Physics D: Applied Physics*, **54**(47), (2021). doi: 10.1088/1361-6463/ac21fe.

[4] M. Ainsli., D. Hu, V. Zermeno, F. Grilli. "Numerical Simulation of the Performance of High-Temperature Superconducting Coils", *J. Superconductivity and Novel Magnetism*, **30**, 1987-1992 (2017). https://doi.org/10.1007/s10948-016-3842-2.

[5] V.M. Krasnov, M. Sandberg and I. Zogaj, "In situ Measurement of Self-Heating in Intrinsic Tunneling Spectroscopy", *Phys. Rev. Lett.*, **94**, 077003 (2005).

[6] HTS Modelling Workgroup. http://www.htsmodelling.com.

[7] F. Rudau et al, "Three-Dimensional Simulations of the Electrothermal and Terahertz Emission Properties of $Bi_2Sr_2CaCu_2O_8$ Intrinsic Josephson Junction Stacks", *Phys. Rev. Appl.*, **5**, 044017 (2016).

[8] V. Krasnov, A. Yurgens, D. Winkler, P. Delsing, "Self-heating in small mesa structures", *J. Appl. Phys.*, **89**, 5578‑5580 (2001).

[9] V.M. Krasnov, "Quantum Cascade Phenomenon in $Bi_2Sr_2CaCu_2O_{8+\delta}$ Single Crystals", *Phys. Rev. Lett.* , **97**, 257003 (2006).

[10] V.M. Krasnov, "Non-equilibrium spectroscopy of high-Tc superconductors", *J. of Phys.: Conf. Ser.* , **150**, 052129 (2009).

[11] V.M. Krasnov, "Temperature dependence of the bulk energy gap in underdoped $Bi_2Sr_2CaCu_2O_{8+\delta}$: Evidence for the mean-field superconducting transition", *Phys. Rev. B.*, **79**(21**)**. (2009).

[12] M.M. Krasnov, N.D. Novikova, R. Cattaneo, A.A. Kalenyuk, V.M. Krasnov. "Design aspects of Bi2Sr2CaCu2O8+ THz sources: optimization of thermal and radiative properties", *Beilstein J. Nanotechnol*, **12,** 1392–1403 (2021). https://doi.org/10.3762/bjnano.12.103.

[13] R. Cattaneo, E. A. Borodianskyi, A. A. Kalenyuk, V. M. Krasnov "Superconducting THz sources with 12% power efficiency", *Phys. Rev. Appl.,* **16**, L061001 (2021). doi: 10.1103/PhysRevApplied.16.L061001, arXiv:2109.00976 [cond-mat.supr-con].

[14] Dorbolo S., Ausloos M. "Influence of a low magnetic field on the thermal diffusivity of Bi-2212", *Phys. rev. B, Condensed matter*, **65**(21) (2002).
[15] R.P. Fedorenko, "A relaxation method for solving elliptic difference equations", *Comput. Math. Math. Phys.*, **1** (4), 1092–1096 (1962).
[16] R.P. Fedorenko, "Iterative methods for elliptic difference equations", *Russ. Math. Surv*., **28**(2), 129–195 (1973).
[17] U. Trottenberg, C.W. Oosterlee, and A. Schuller, *Multigrid*, Academic, New York, (2001).
[18] V.T. Zhukov, N. D. Novikova, O. B. Feodoritova, "Multigrid method for elliptic equations with anisotropic discontinuous coefficients", *Comput. Math. Math. Phys.*, **55** (7), 1150–1163 (2015).
[19] V.T. Zhukov, N.D. Novikova, O.B. Feodoritova, "On the Solution of Evolution Equations Based on Multigrid and Explicit Iterative Methods", *Comput. Math. Math. Phys.*, **55** (8), 1276–1289 (2015).
[20] V.T. Zhukov, N.D. Novikova, O.B. Feodoritova, "Parallel multigrid method for solving elliptic equations", *Math. Models Comput. Simul.* **6**(4), 425–434 (2014).
[21] V.T. Zhukov, N.D. Novikova, OB. Feodoritova, "Multigrid method for anisotropic diffusion equations based on adaptive Chebyshev smoothers", *Math. Montis.*, **36**, 14–26 (2016).
[22] O.B. Feodoritova, M.M. Krasnov, V.T Zhukov, "Adaptive technique for Chebyshev-based solvers for three-dimensional elliptic equations", J. Phys: Conf. Ser., 012012 (2018).
[23] O.B. Feodoritova, V.T. Zhukov, "An adaptive multigrid on block-structured grids", *J. Phys.:Conf.Ser.*, 1640012020 (2020). doi:10.1088/1742-6596/1640/1/012020.
[24] A.A. Samarskii, E.S. Nikolaev, *Numerical Methods for Grid Equations, v.1 Direct Methods, v.2 Iterative Methods*. Birkhauser Verlag, Basel, Boston, Berlin. (1989).
[25] F. R. Gantmacher, *The Theory of Matrices*. Chelsea, New York. (1959).
[26] E. Zipunova, E. Savenkov, "Phase field model for electrically induced damage using microforce theory", *Math. and Mechanics of Solids*, (2021). doi:10.1177/10812865211052078.
[27] E. Zipunova, E. Savenkov,"On the Diffuse Interface Models for High Codimension Dispersed Inclusions", *Mathematics*, **9**(18). 2206.(2021) https://doi.org/10.3390/math9182206.

Received, December 20, 2021